

Optimum mirror shapes and supports for light weight mirrors subjected to self-weight

Myung K. Cho, Ralph M. Richard, and Daniel Vukobratovich

Optical Sciences Center
University of Arizona
Tucson, Arizona 85721

ABSTRACT

A parametric design study of light weight mirror shapes with various support conditions was performed utilizing the finite element program NASTRAN. Improvements in the mirror performance were made based on the following design criteria: (1) minimization of the optical surface wavefront variations, (2) minimization of the self-weight directly related to cost of manufacturing, and (3) optimal location of support points. A pre-processor to automatically generate a finite element model for each mirror geometry was developed in order to obtain the structural deformations systematically. Additionally, a post-processor, which prepares an input data file for FRINGE (*an optical computer code*) was developed for generating the optical deflections that lead to the surface wavefront variations. Procedures and modeling techniques to achieve the optimum (*the lightest and stiffest mirror shape due to self-weight*) are addressed.

1. INTRODUCTION

Gravitational deflections for a mirror with its optical axis horizontal, vertical, or in an arbitrary orientation are generally required for design of an optical system. Typical conventional mirrors are usually massive so that associated self-weight deflections are the cause of the optical wavefront errors. Numerous theoretical and analytical efforts in opto-mechanical engineering have been devoted to minimizing self-weight deflections by either reducing weight and/or optimizing support systems. Parameters behind the methodology applied during the design process involve the optical performance specification and the definition of imposed constraints. It is often necessary to perform parametric analyses in order to develop the correlations between design characteristics. Once the structural analysis of a mirror has been achieved, an evaluation of the optical performance is required. Based on the imposed error budget and design requirements, which define the RMS variation over the optical surface, the best mirror configuration can be selected. In this research, a parametric mirror shape study was conducted. Improvements in the optical performance were made based on the minimizing the self-weight deflections, optimizing support locations, and imposed optical constraints.

2. PRE- AND POST-PROCESSORS

Procedures to evaluate the effects of the performance of optical mirrors due to gravity load have been developed at the Optical Sciences Center of the University of Arizona. These methodologies involve the implementation of finite element programs and the optical program FRINGE.¹ The FRINGE program is utilized to quantitatively estimate the characteristics of optical surfaces from either test data or finite element analyses. Iraninejad *et. al.*,² modified the FRINGE program to accept as its input, the selected output from the structural analysis finite element program SAP IV. The current version of FRINGE has been further modified by the authors in order to accept the output from the structural analysis program NASTRAN. Thus structural deflections over the optical surface, which are output from the finite element program NASTRAN, then become the input to program FRINGE which performs a wavefront error analysis.

2.1. Pre-processor

The major effort in finite element modeling is defining the geometry of the structure. For a complicated three dimensional structure, a tremendous amount of time and effort may be required. Thus a generic shape equation which can define mirror shape contours is extremely useful. In this paper, a pre-processor with a generic mirror contour shape equation was written, which produces a NASTRAN input data file based on the generic shape equation. The processor is made up of three programs - EQN, MPROP, and MGEN3D. Program EQN calculates parameters of each contour shape, identifies the shape, and then stores the generic shape equation. The generic equation is given by

$$Y = A + B (C - X^2)^{\frac{1}{2}} + \frac{1}{D} (X - E)^G + F X \quad (1)$$

Parameters in Equation (1) generate circular, parabolic, linear, and combinations of these shapes for each mirror. Through this routine, a database for each mirror shape is established.

Program MPROP uses the shape equations of the database and determines the properties such as cross sectional area, mirror weight, location of the center of gravity, mass moments of inertia, and geometry of the section. The mirror geometry can be plotted and examined in this stage before going into actual structural analysis. Once this geometry has been determined, program MGEN3D is used to generate the three dimensional mesh mirror models for NASTRAN. Mirror geometry and finite elements are generated in accordance with contour equations in the database.

The attributes of this pre-processor are the followings: (1) all three routines can be either run separately or linked together by a means of a batch command, (2) control data files for the routines are easy and simple to prepare, (3) the database can hold as many as 1000 contour shape equations, and (4) geometry of each mirror model can be previewed prior to making a structural analysis.

2.2. Post-processor

Surface distortion over the mirror controls the qualitative performance of the optical system. For optical design purposes, the wavefront errors are required in terms of the components such as tilt, defocus, astigmatism, coma, spherical, trefoil, and other common aberrations. Program FRINGE, an optical program, was used to generate a least square fit of Zernike polynomials to the deformed surface to evaluate the optical quality.

Either a one sixth model (60 degrees) or a one half model of a mirror (180 degrees) was utilized depending upon the symmetry of the support systems and the loading conditions. The post-processor consists of the two computer programs, TRANS and FRINGE. Program TRANS uses output from NASTRAN, and selects information about the geometry and the displacement components over the surface of the mirror for input data to FRINGE. During the conversion procedure, the symmetry was applied. At this stage the deformed shape can be viewed and evaluated. Program FRINGE provides the peak to peak variation, RMS wavefront error, deformation contours, the spot diagram, and the radial energy distribution. Shown in Figure 1 is a flow diagram of procedure used in this research.

3. CONVENTIONAL MIRROR ANALYSIS

In general, mirrors may be classified in accordance with the contour of the back surface. A plate with uniform thickness is one of the simplest mirrors, and it is the classical or conventional mirror model. A concave mirror with a flat back, a meniscus mirror, and a double concave mirror fall into the same category. Figure 2 (a) shows a concave flat back mirror which is not light weighted. Shown in Figure 2 (b) is a meniscus mirror whose back surface has the same contour as the optical surface. Figure 2 (c) represents a double concave mirror which has a convex back contour. Shown in Figure 2 (d) is a tapered back mirror with a straight contour. The mirror in Figure 2 (e) is a convex back mirror with a parabolic contour. Mirrors in Figures 2 (f) and (g)

represent single and double arch mirrors with parabolic contours. Figures 2 (a), (b) and (c) show mirror shapes that are regarded as conventional whereas Figures (d) through (g) show light weighted contour shapes. In this section the conventional mirror shapes, the first three in Figure 2, are analyzed. The light weighted mirrors will be treated in sections 4 and 5.

Each contoured back shape was analyzed for the following five support systems: (1) a ring support, (2) twelve equally spaced supports at 30 degrees denoted as 12-30, (3) six equally spaced supports at 60 degrees denoted as 6-60, (4) four equally spaced supports at 90 degrees denoted as 4-90, and (5) three equally spaced supports at 120 degrees denoted as 3-120. Each contoured back mirror was 40 inches in diameter, with a radius of curvature of 160 inches, and an outer edge thickness of 5.0 inches. The reason for the limit on the thickness is that for an optical glass, for example Corning code 7940 fused silica, a circular blank can be manufactured up to 5.0 inch thickness without material inhomogeneity. Support ratios (r/R_o) ranging from 0.1 to 1.0 were made for each support system. Additionally, two extreme mirror orientations, which are the optical axis vertical (ZENITH) and the optical axis horizontal (HORIZON), are considered for each support condition. For the HORIZON case, the mirror is always supported at the center of the gravity for all analyses.

3.1. Concave flat back mirror

A 40 inch diameter f/2.0 concave flat back mirror model made out of SXA was used to estimate the effect of thickness variation. SXA, an aluminum and silicon carbide metal matrix composite, has the following material properties:

Elastic modulus = 16.0×10^6 psi
Poisson's ratio = 0.30
Weight density = 0.10 lb/in³

The concave back shape was regarded as a "baseline", and the surface deformations were evaluated. Table 1 shows the optical surface RMS wavefront error versus the support ratio for the support systems. The RMS values for lower support ratios, ranging from 0.1 to 0.4, are not sensitive for the support systems in ZENITH position whereas larger RMS variations are found as r/R_o increases. Comparing support systems 4-90 and 3-120, for example, more than a factor two in RMS is observed in the case of $r/R_o=1.0$. In the HORIZON position, however, surface deformations do not change significantly for these support systems. In Figure 3 is shown the RMS wavefront error versus support ratio for the five support systems in ZENITH. Since the RMS values for both the ring and 12-30 supports are practically identical, these plots are given in a single curve. For this particular shape of mirror, the lowest RMS wavefront error results when either the ring support or 12-30 support system is at about 0.6 radius. If the 3-120 support system is a design requirement, then the optical structure needs to be supported at about 0.5 radius to get the optimum optical performance. Through these analyses it is found that the optimum support location depends on the support systems, and the support ratio lies between 0.5 and 0.6 for all the concave flat back mirrors.

3.2. Meniscus mirror

A 40 inch aperture, f/2.0 meniscus SXA mirror with a uniform thickness of 5.0 inches was analyzed to examine the effect of contoured back shapes. The weight of this shape is 620 pounds. As the previous analyses, five support systems with both orientations are considered with exception of support locations. The meniscus mirror is now supported at the outer edge ($r/R_o=1.0$). The optical performance in RMS variation is given in Table 2.

3.3. Double concave mirror

A 40 inch SXA mirror with both the optical and back surfaces concave and supported at the outer edge ($r/R_o=1.0$) was analyzed. The same radius of curvature of 160 inches with an outer edge

thickness of 5.0 inches, labelled as configuration 1, was used. Evaluation of the optical performance for this configuration was made with various boundary conditions. In order to examine the effect of the thickness of the mirror, another configuration with an outer thickness of 4.0 inches and inner of 1.6 inches, labelled as configuration 2, was analyzed as well. A comparison between those configurations has been made and listed in Table 3. As shown in the table, the reduction of the thickness and 25 percent of the self-weight increased the RMS wavefront errors by about 60 percents in ZENITH position but remained unchanged in HORIZON. If the mirror is to be used in HORIZON position, it would be acceptable to reduce the thickness for this double concave shape. Again, this mirror was supported at the center of the gravity for the HORIZON position.

4. LIGHT WEIGHT MIRROR ANALYSES

Minimizing self-weight deflections of a mirror by reducing its self-weight or optimizing support systems has been attempted by many researchers. Generally, lightweighting a mirror guarantees better optical performance if it is properly supported. Figures 2 (d) through (g) show typical light weight mirrors.

4.1. Single arch mirror analysis

A 40 inch single arch SXA mirror with a maximum depth of 5.0 inches was analyzed. As shown in Figure 4, the mirror has a 4.0 inch diameter central hole, an outer edge thickness of 0.5 inches, and a 2.0 inch land. The self-weight was 135 pounds and it was supported at $r/R_o=0.15$. The optical performance data is listed in Table 4. Shape studies on single arch and single arch like mirrors with contours such as straight tapered back, and convex back will be discussed in detail in the next section.

4.2. Double arch and double arch like mirror designs

The attributes of a double arch shape are (1) excellent stiffness to weight ratio, (2) ease in fabrication, (3) design flexibility of the support system, (4) relatively good mass distribution to mirror orientation, and (5) resistance in torsional excitation. A primary 40 inch mirror with a focal ratio $f/2$, was selected for a trade study between cost and performance. The maximum depth of the primary mirror was 5.0 inches as in earlier analyses.

Four basic mirror back shapes of these 40 inch SXA mirrors with various support conditions were considered. Each of them has a distinctive back contour, but has the same inner edge thickness of 0.5 inches and outer edge of 0.5 inches. The radius of curvature was set at 160 inches for all mirrors. Typical cross sections of the basic shapes and the parameters of each back contour defined by Equation (1) are shown in Figure 5. A typical finite element model for a 40 inch double arch mirror is shown in Figure 6. The deformed shape of the surface of the mirror with 3-120 support in ZENITH position is shown in Figure 7. Radial deflections of each mirror surface, plotted for the different support ratios in ZENITH position, are shown in Figure 8. Figure 8 (a), for example, shows the structural deflections of each contoured back shape supported at $r/R_o=0.50$ radius. The optical surface performance in terms of RMS wavefront errors are listed in Tables 5 through 8. For $r/R_o=0.50$ shown in Figure 8 (a), the contour shape (EQN 2-3) shows the smallest variation in slope of the deflected surface whereas (EQN 4-5) has the largest. Models identified as (EQN 2-3 and 6-7) produced the RMS wavefront errors of 0.021 waves at $r/R_o=0.50$ with a ring support. For a ring support at 0.55 radius, the lowest RMS is found from (EQN 6-7) in ZENITH position. The value is well below that from (EQN 1-2) which produced the least slope variation of the deflected optical surface as shown in Figure 8 (b). A similar pattern is also observed for (EQN 4-5) with $r/R_o=0.60$. It is apparent that there is no precise correlation between the slope of the deflected surface and the RMS wavefront error; however, the variation in the slope of the surface gives a reasonable indication of the actual optical performance.

Figure 9 shows that the optimum support position varies for contoured back shapes in ZENITH position. For a ring and a 6-60 support systems as shown in Figures 9 (a) and (b), the best

optical performance can be obtained when the contoured back shape of (EQN 6-7) is supported at 0.55 radius. Figure 9 (c) shows that an optimum support position for the shape of (EQN 4-5) is found when it is supported by 4-90 support system at 0.55 radius while both shapes of (EQN 1-2) and (EQN 6-7) should be supported at less than 0.5 radius. For a 3-120 support shown in Figure 9 (d), on the other hand, supports at less than 0.5 radius are the best regardless of the contour shapes. These plots give an indication where support systems should be located. It is noted that the RMS value is strongly dependent upon contour back shape and support system.

To examine the effects of material properties, a 40 inch mirror made of Corning code 7940 was analyzed. This fused silica has the following material properties:

Elastic modulus = 10.7×10^6 psi
Poisson's ratio = 0.17
Weight density = 0.092 lb/in³

The mirror has the same configuration as (EQN 6-7) with $r/R_o=0.5$. Summarized in Table 9 is a comparison of the SXA and fused silica 40 inch mirror results. The RMS wavefront errors for both materials are not affected significantly for support systems of the ring, 12-30, and 6-60 in ZENITH position. The fused silica mirror had about 30 or 40 percent higher RMS values for support systems of the 4-90 and 3-120. The reason is that surface deflection is a function of specific stiffness (weight density to Elastic modulus ratio). The evaluations of optical performance of various contoured back shapes addressed in this section are summarized and listed as Table 10. The RMS values of the concave flat and double arched (EQN 2-3) mirrors are listed only for $r/R_o=0.6$.

5. SINGLE ARCH AND SINGLE ARCH LIKE MIRROR ANALYSES

A study of a 16 inch $f/1.5$ primary mirror was performed to achieve both minimum weight and surface deformation. In this design study, single arch and single arch like contoured back shapes (*tapered straight back, convex back, parabolic curved back, and combined curved back*) were used. Each mirror had maximum depth of three inches, an outer edge thickness of 0.25 inches, and a ring support at the inner radius for both ZENITH and HORIZON positions.

5.1. Solid SXA mirror

Eight solid SXA 16 inch mirrors with various back contour shapes were considered. In order to examine the sensitivity of radius of curvature of the mirror, mirror models with flat and concave surfaces were used. For the concave surface model, the radius of curvature of the mirror was 48 inches. Typical contoured back shapes are shown in Figure 10. Shown in Table 11 are the performances due to self-weight for the optical axis in the vertical and horizontal positions.

Mirrors identified by SXA13 through SXA15 had flat optical surfaces, whereas a radius of curvature of 48 inches was used for the others. SXA13, a typical single arch contoured back as shown in Figure 10 (a), gave the lowest RMS values of both HORIZON and ZENITH among all the shapes. SXA14, a straight back contour in (b) of the same figure, had not only the lowest RMS value in HORIZON but a relatively low RMS in ZENITH. Among flat optical surface mirrors, SXA15, a parabolic contoured back which produces a constant radial bending stress^{3 4} and illustrated in Figure 10 (c), showed the largest surface distortions in both mirror positions and was the heaviest. SXA23, the same back shape as SXA13 with a concaved optical surface, had higher values of RMS wavefront errors but was the lightest. This model, however, has a thickness inside the outer edge, which is thinner than that at the edge of the mirror because of the concave optical surface. SXA24, had the same back shape as SXA14. SXA 25 shown in Figure 10 (c) uses the same contoured back shape as SXA15. SXA29 shown in Figure 10 (d), a version of SXA23 (*a combined back shape of an arch and a higher order contour revised to eliminate the thin interior section*), had essentially the same RMS values for both positions. From the standpoint of reduction of the self-weight, this would be the best choice, however there are some trade-offs. First, it has a discontinuity in the contour of the back which may cause difficulties during manufacturing process. Next, the optical performance of this model

turned out to be the worst in HORIZON and ZENITH. SXA30, a modified single arch model illustrated in Figure 10 (e), showed the lowest RMS in HORIZON as well as relatively low in ZENITH. If the lowest weight and RMS wavefront error in HORIZON were the design requirements, the best configuration would be SXA30. A finite element model of this configuration is shown in Figure 11.

5.2. SXA foam mirror

The use of foamed metals and ceramics as core materials in light weight structural applications has been of interest in recent years. Material properties of the composite structures, however, are difficult to accurately establish because of the variables associated with foam materials. The foam core is usually bonded to face plates which are relatively thin; therefore, the core resists shear force whereas the face plates resist flexural forces. The overall structural deformation of the foam mirror is a combination of flexural and shear deformation. Tests ⁵ were made to determine the shear modulus for a SXA foam and a nickel foam which controls the structural deformation of a composite foam.

As a demonstration of the potential of foam core mirror technology, a 12 inch aperture, f/5.0 Cassegrain telescope weighing ten pounds was recently designed and fabricated at the University of Arizona Optical Sciences Center.⁶ The telescope was designed with a primary mirror composed of aluminum face plates and aluminum foam composite. Aluminum foam core mirrors with aluminum face plates have been produced using dip brazing to attach the core to the face plates. A comparison between the finite element analysis and the test of the aluminum foam core mirror was made by Pollard.⁷ In that paper, the authors found that the discrepancy between the actual and analytically predicted performance of the optical surface was significant. They attributed this to the lack of accurate material properties of the aluminum foam core. Moreover, for applications requiring surface precision greater than about 630 nm (nano meter) RMS, aluminum is questionable because of its dimensional instability.

A design study of a 16 inch primary foam mirror was made to determine an optimum contoured back shape as well. The same geometries were applied for the foam mirrors as for the SXA solid mirrors. A SXA foam with 10 percent density of solid SXA, an aluminum and silicon carbide metal matrix composite, and nickel foam with 2 percent density were analyzed. The following are the material properties of the SXA foam and the nickel foam.

	SXA FOAM	NICKEL FOAM
Elastic modulus	13,000 psi	4,000 psi
Shear modulus	6,500 psi	2,000 psi
Weight density	0.01 lb/in ³	0.0062 lb/in ³

Six contoured mirrors with different foam core materials were analyzed. Each had SXA face plates of 0.125 inches for both the front and the back surfaces. Shown in Table 12 are the optical performances due to its self-weight in both ZENITH and HORIZON positions. In addition, the overall weight and the foam core weight ratio of each mirror are listed in the table.

SXA face plates with an SXA foam core were used for mirrors of SW27 through SW31, whereas SXA face plates with a nickel foam core were used for SW40. Typical contoured back shapes are shown in Figure 10. SW27, a single arch mirror shown in Figure 10 (a), gave the highest RMS value in HORIZON among the SXA foam core mirrors. SW28, a much stiffer version of SW27, reduced the RMS distortion by 15 percent in HORIZON but increased it by four percent in ZENITH. A straight back shape which is SW29, the heaviest shape shown in Figure 10 (b), had the lowest RMS value in HORIZON but the highest in ZENITH. A parabolic back shape illustrated in Figure 10 (e), SW30, gave an intermediate RMS value in HORIZON and the lowest in ZENITH, and it weighed only 7 pounds. SW31, a straight back type, had higher RMS values. SW40, the same shape as SW30, was made of a nickel foam which had a lower shear modulus and weight density than the SXA foam. SW30 in comparison with SW40 which had 15 percent less self-weight gave about 80 percent higher RMS distortion. This shows that the shear modulus of a form core material has a significant effect

on the optical surface quality. Provided that a 0.1 RMS wavefront error in HORIZON and the lowest RMS in ZENITH were the design requirements, the optimum configuration would be SW30.

6. CONCLUSIONS

A parametric design study of light weight mirrors has been made based on the following design constraints:

- 1) Gravitational load applied both in ZENITH and HORIZON;
- 2) A 40 inch mirror with a total depth of 5.0 inches and a radius of curvature of 160 inches;
- 3) A 16 inch mirror with a total depth of 3.0 inches and a radius of curvature of 48 inches;
- 4) For the HORIZON position, the mirror was supported its center of gravity.

Through examining various contoured back shapes based on the imposed design constraints, the following conclusions were drawn:

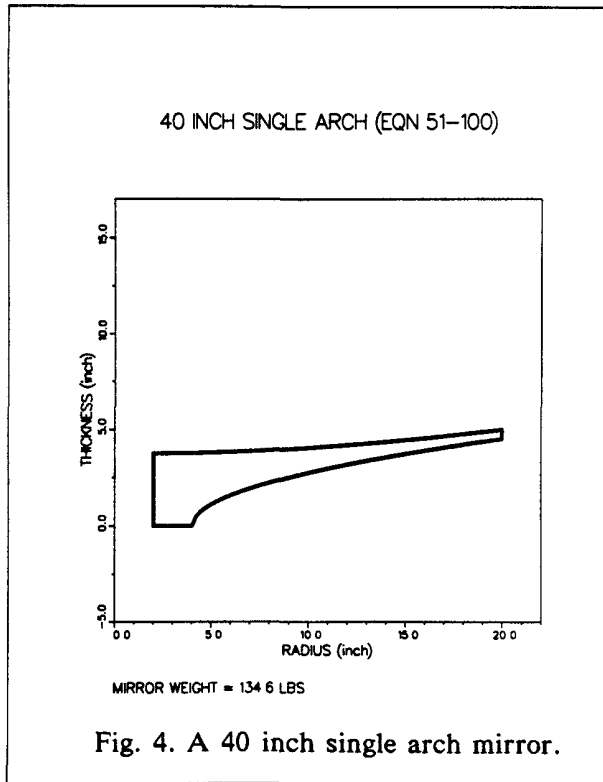
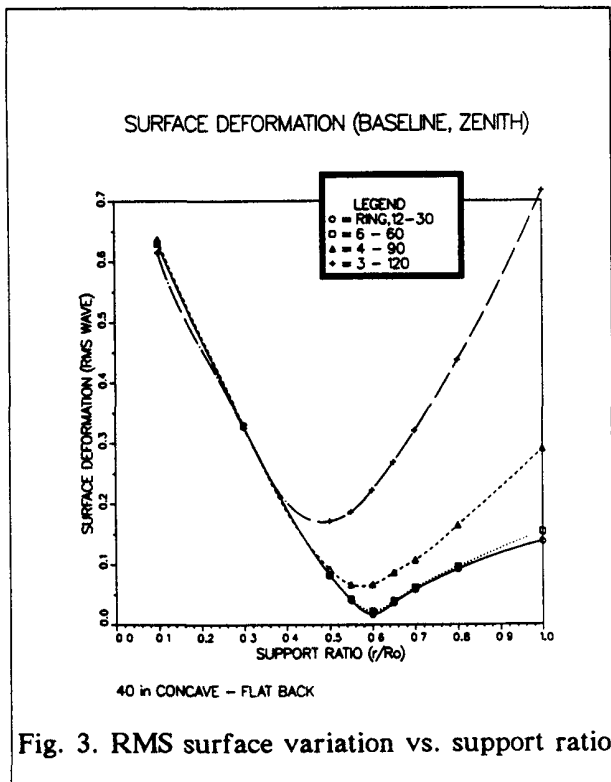
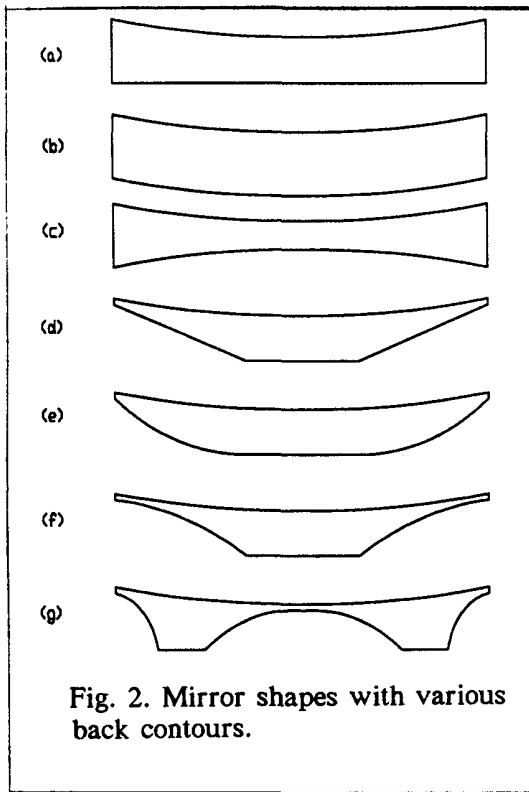
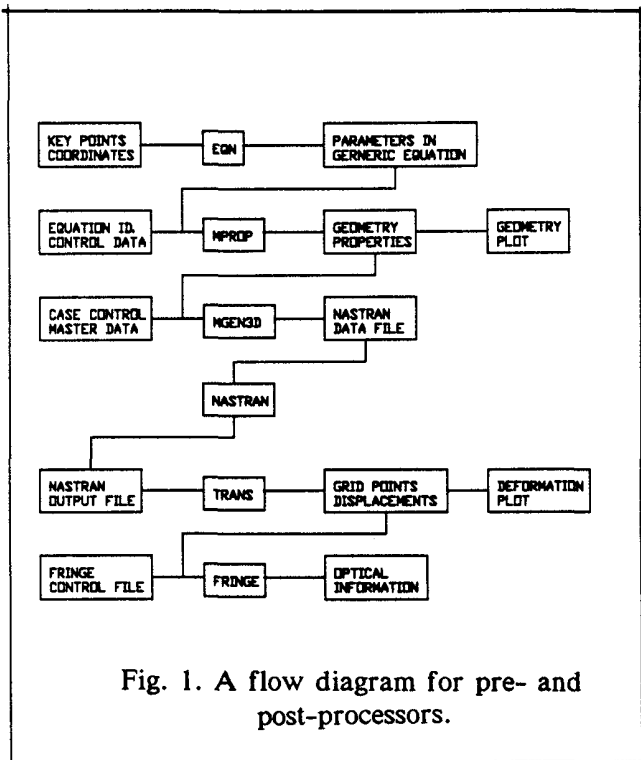
- 1) The optical performances were very sensitive to the material parameters, contoured back shape, and support location;
- 2) There was not a precise correlation between the slope variation of a deflected surface and the optical RMS wavefront errors; however, the slope variation of the deflected surface may be used as a first order approximation to the optical performance;
- 3) An optimum shape of a double arch mirror for a ring support at 0.55 radius was found with the contoured back shape of (EQN 6-7);
- 4) An optimum location for a three equally spaced support system was smaller than 0.5 radius regardless of the contoured back shapes;
- 5) For a single arch mirror supported by a ring, the optimum shape was a parabolic contour with the vertex at the base of the mirror, which was used for SXA30 and SW30.

7. ACKNOWLEDGEMENT

This Study was partially supported by NASA Ames Research Center through the NASA Cooperative Agreement NAG2-426 with the University of Arizona. The authors wish to acknowledge Ramsey Melugin, the technical monitor of the program at the NASA Ames, for his helpful comments and suggestions.

8. REFERENCES

1. Anderson, D., *FRINGE Manual*, Version 3, Optical Sciences Center, University of Arizona, Tucson, Arizona, April 1982.
2. Iraninejad, B. and Vukobratovich, D., *Double Arch Mirror Study*, Engineering Analysis report, NASA Grant 2-220, NASA Ames Research Center, Mail Stop 244-7, Moffett Field, California 94035, Mary 1983.
3. Lee, J. P., *Approximate Solutions of Circular Plates of Constant Radial Bending Stress*, Developments in Theoretical and Applied Mechanics, Proceedings of the Ninth Southeast Conference on Theoretical and Applied Mechanics, May 1971.
4. Lee, J. P., *Symmetrical Bending of Circular Plates of Constant Radial Bending Stress*, Journal of Applied Mechanics, No. 12, December 1962.
5. Stone, R. M., *Shear Moduli for Cellular Foam Materials*, Masters Thesis, University of Arizona, Tucson, 1989.
6. Vukobratovich, D., *Lightweight Laser Communications Mirrors made with Metal Foam Cores*, Proceedings of SPIE, Vol. 1044, 1989.
7. Pollard, L. W., Vukobratovich, D., and Richard R. M., *The Structural Analysis of a Light-Weight Aluminum Foam Core Mirror*, Proceedings of SPIE, Vol. 748, 1987.



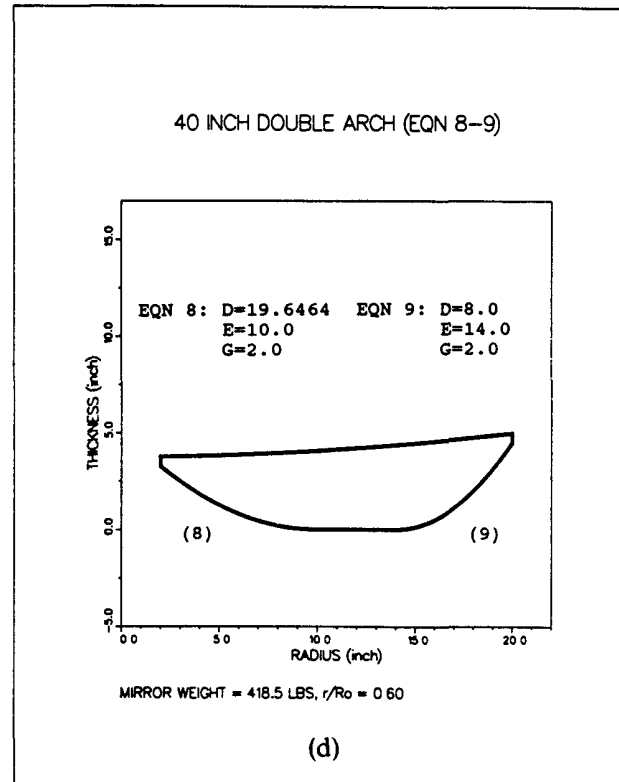
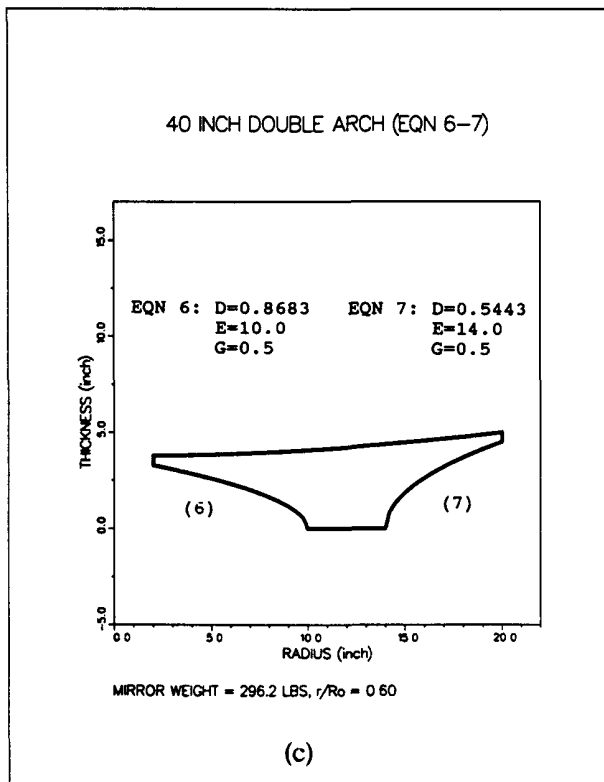
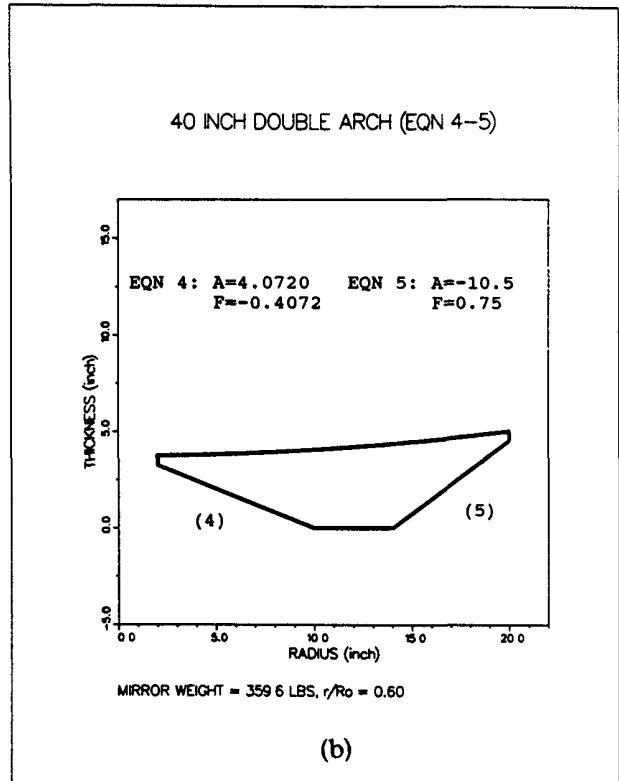
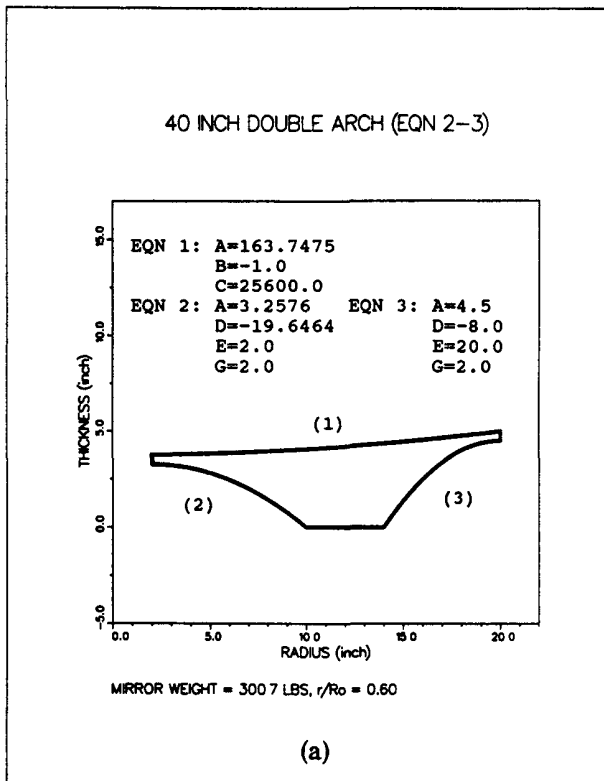


Fig. 5. 40 inch double arch and double arch like shape mirrors.

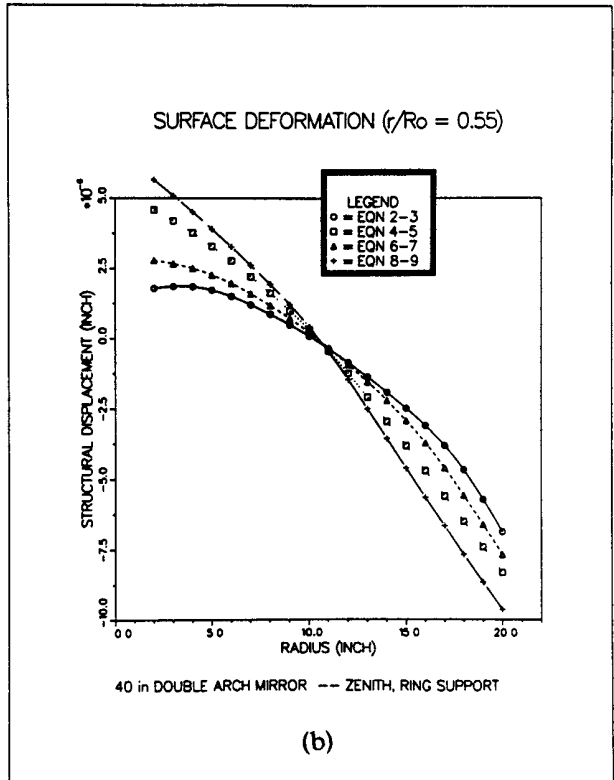
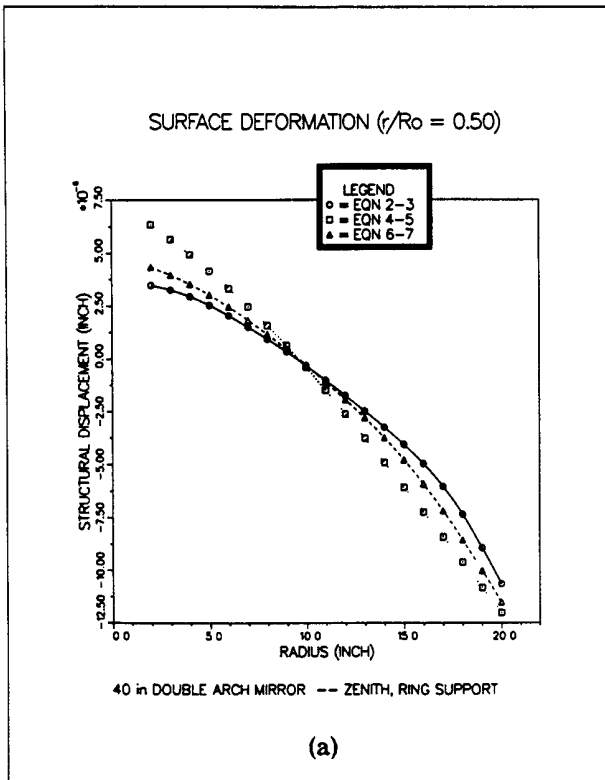
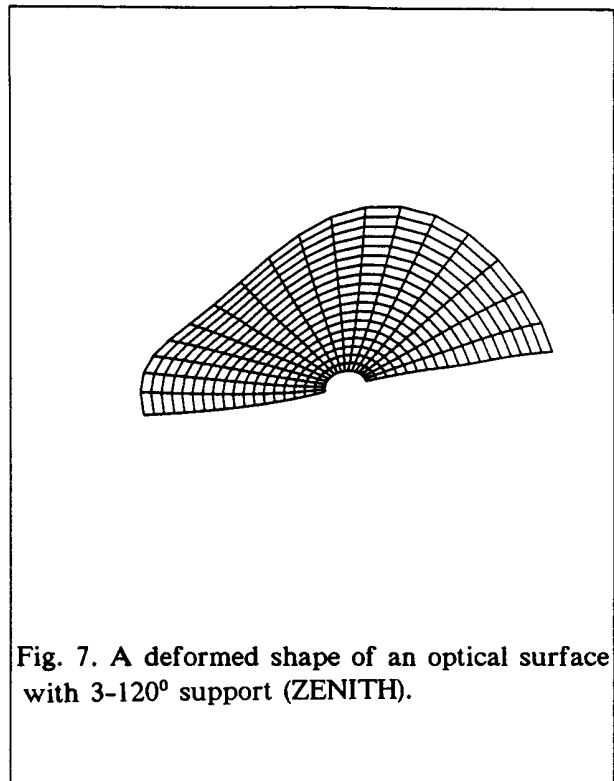
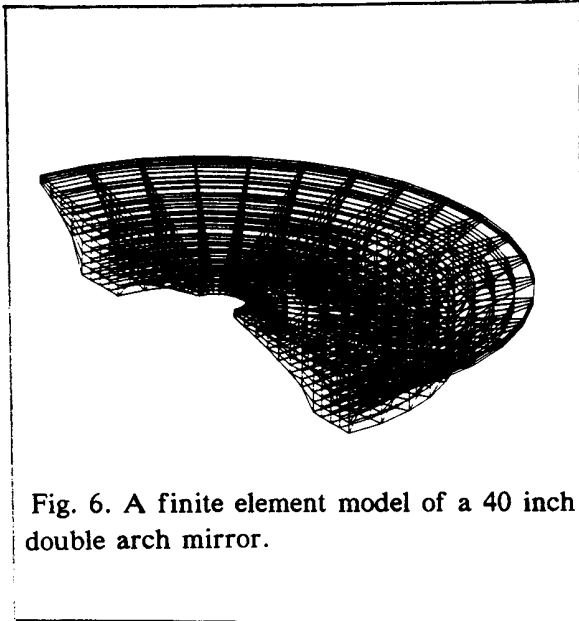


Fig. 8. Structural Deflections with a ring support (ZENITH).

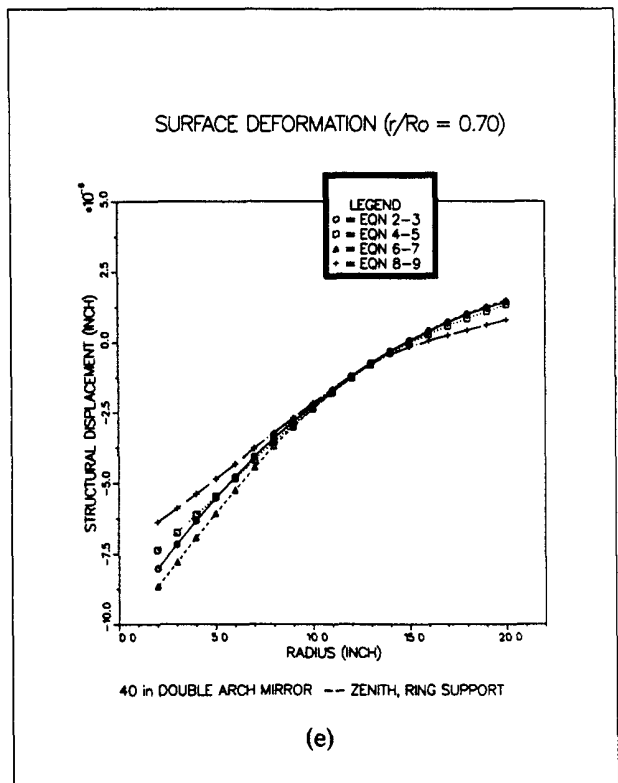
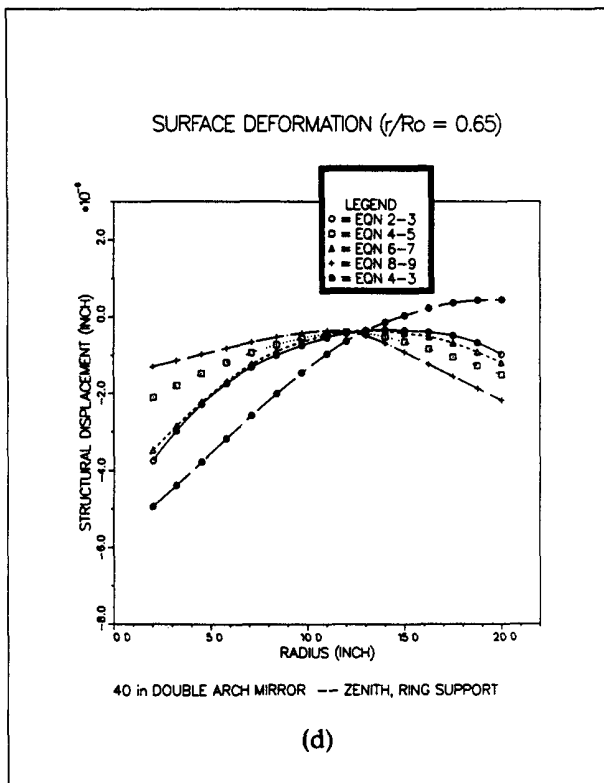
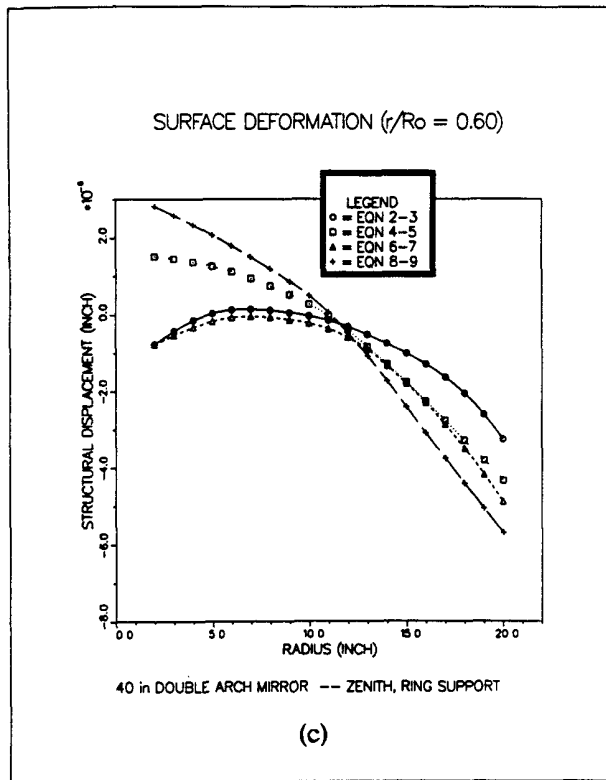


Fig. 8. Structural Deflections with a ring support (ZENITH).

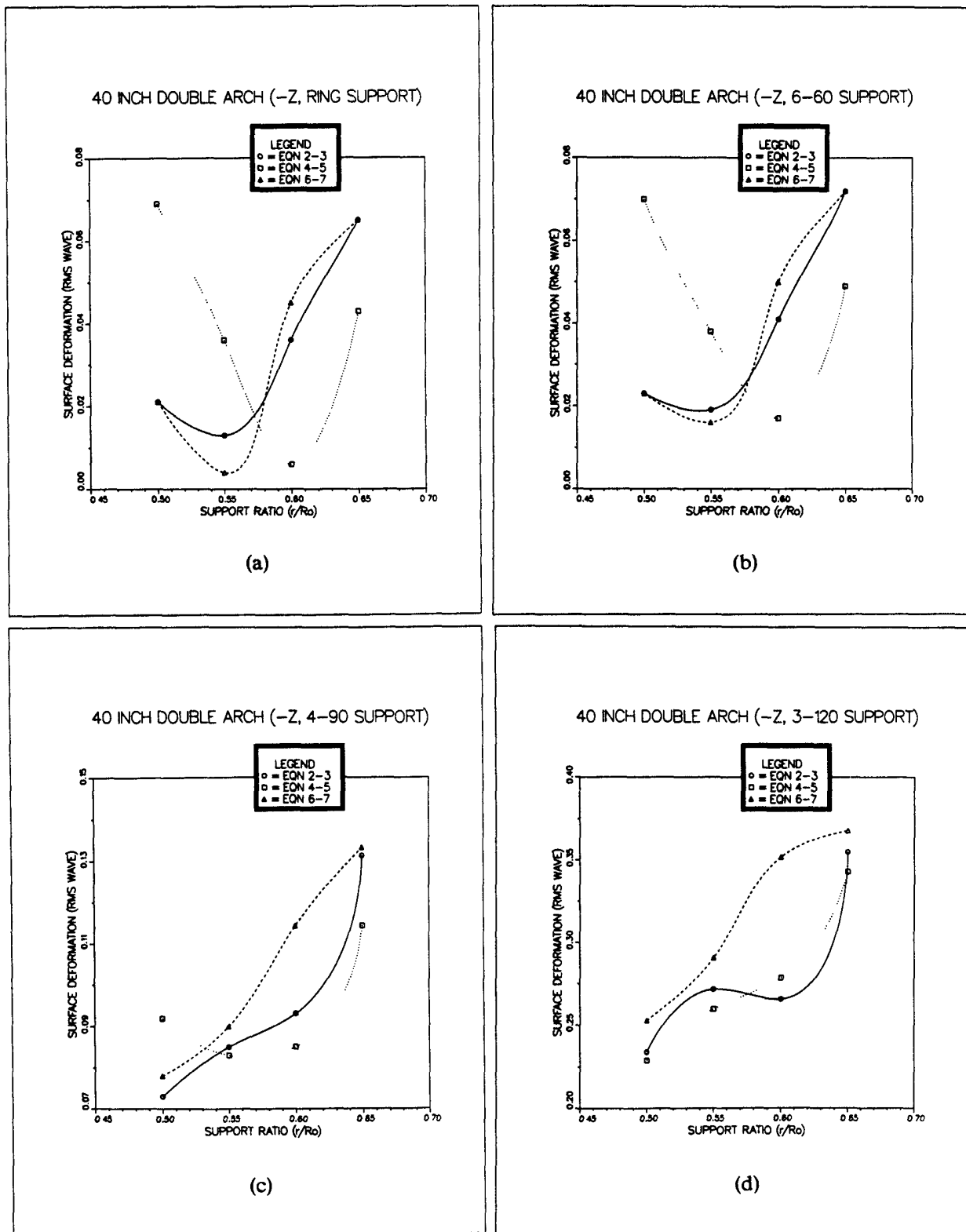


Fig. 9. RMS surface variation vs. support ratio (ZENITH).

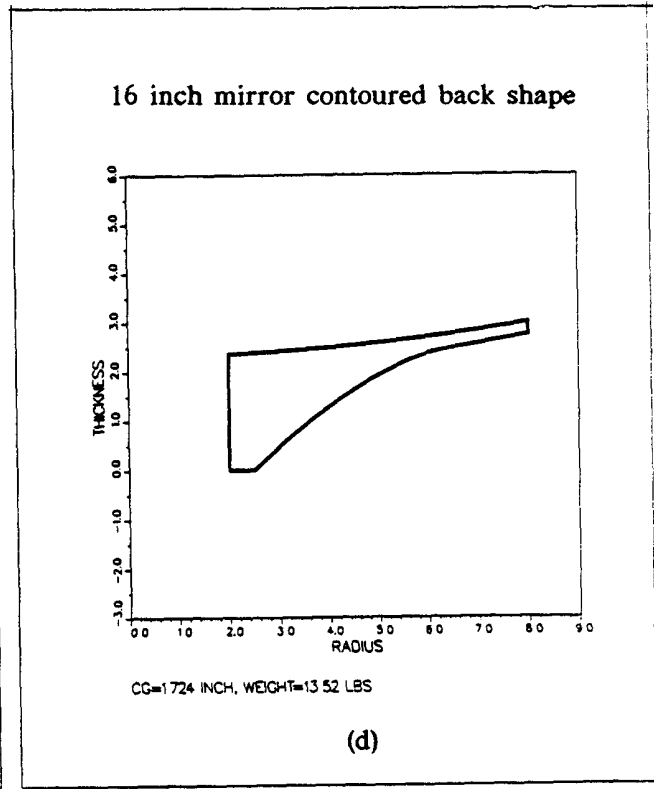
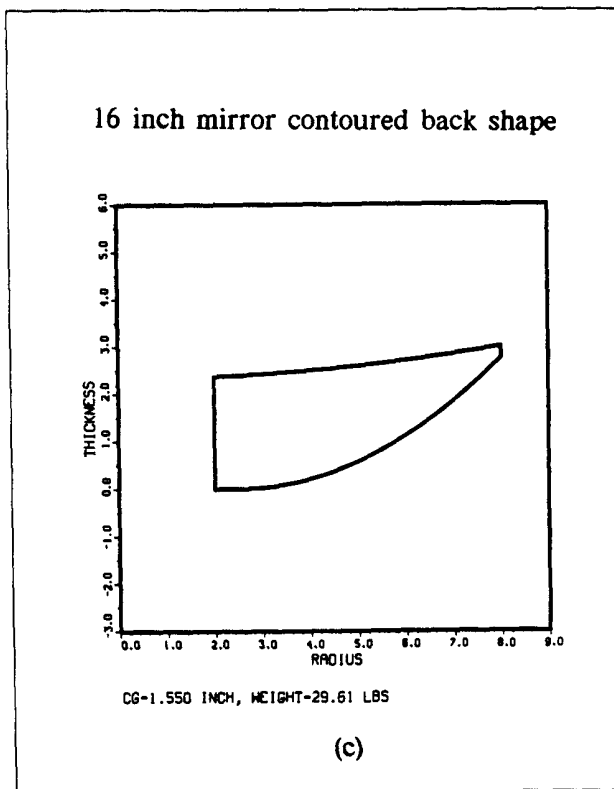
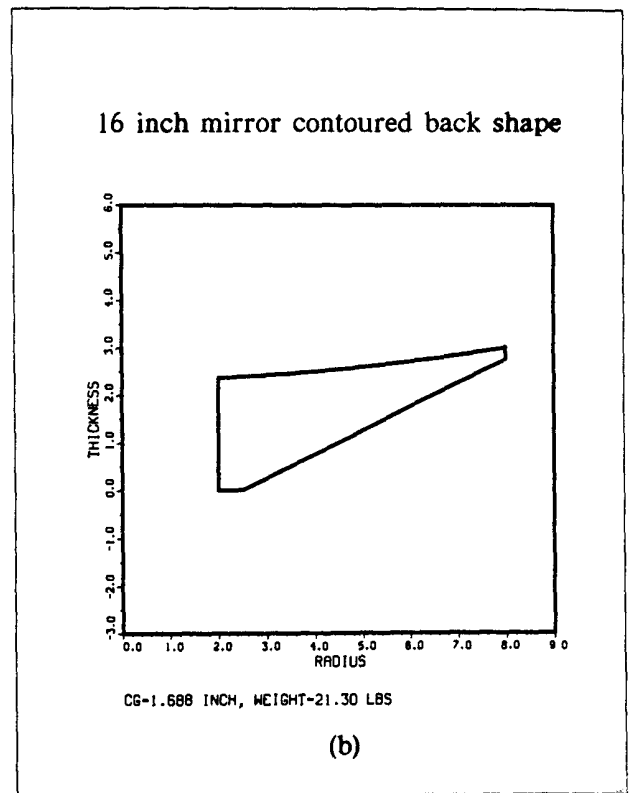
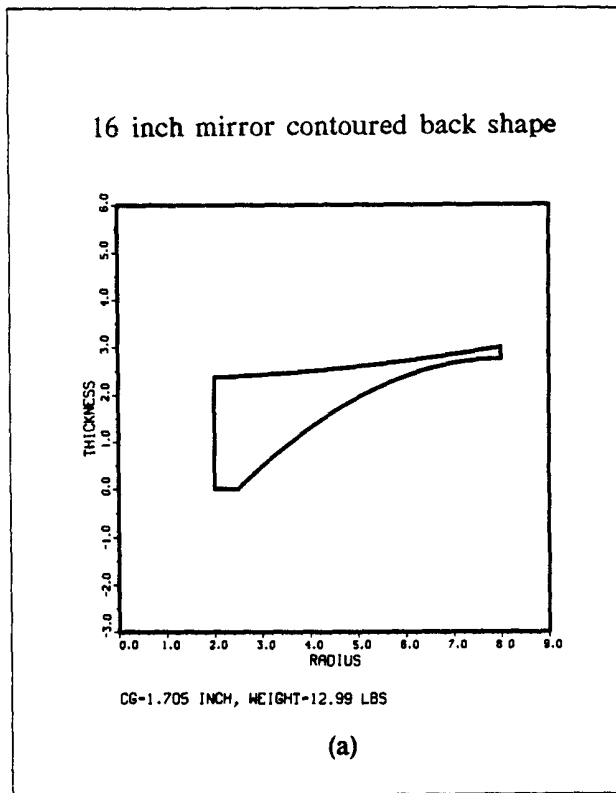


Fig. 10. 16 inch single arch and single arch like shape mirrors.

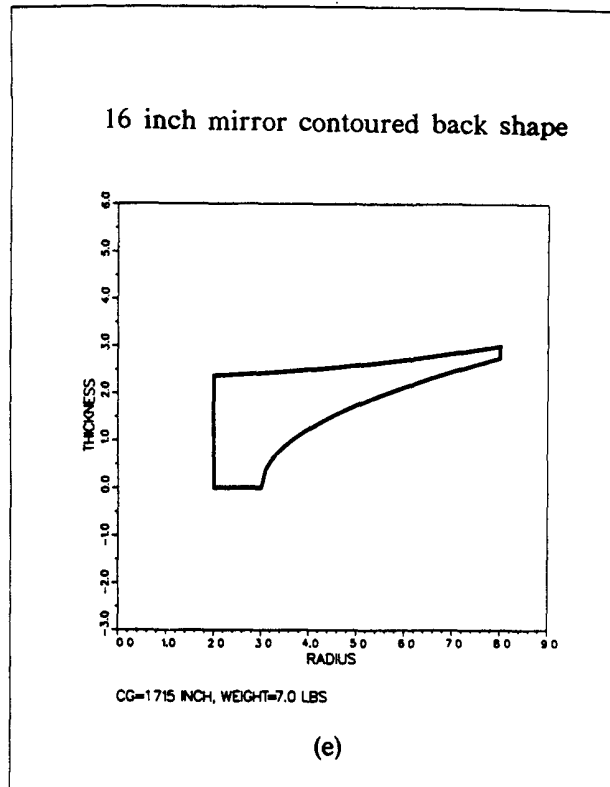


Fig. 10. 16 inch single arch and single arch like shape mirrors.

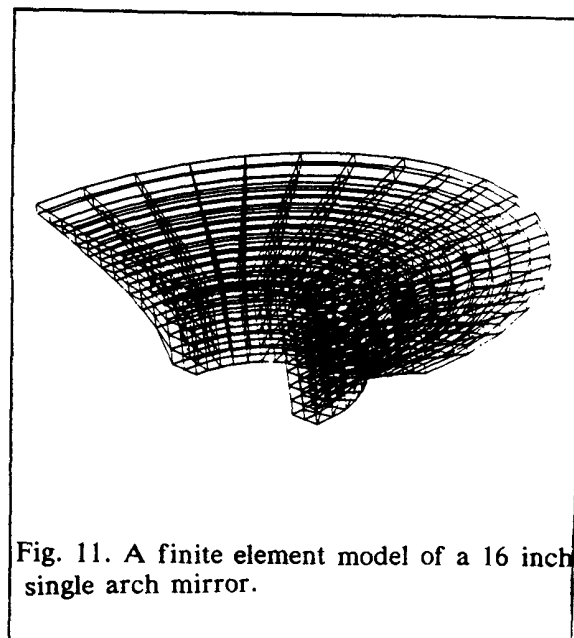


Table 1. 40 inch SXA mirror baseline (Concave-Flat)

SUPPORT r/Ro	GRAVITY LOAD	----- SURFACE DEFORMATION (RMS WAVE) -----				
		RING	12-30	6-60	4-90	3-120
0.10	ZENITH	0.630	0.630	0.631	0.637	0.620
0.30	ZENITH	0.328	0.328	0.329	0.330	0.326
0.50	ZENITH	0.082	0.082	0.084	0.091	0.171
0.55	ZENITH	0.040	0.041	0.042	0.066	0.186
0.60	ZENITH	0.017	0.018	0.022	0.066	0.222
0.65	ZENITH	0.036	0.037	0.039	0.086	0.268
0.70	ZENITH	0.058	0.059	0.061	0.107	0.320
0.80	ZENITH	0.092	0.093	0.096	0.164	0.437
1.00	ZENITH	0.138	0.140	0.154	0.290	0.717
--	HORIZON	0.028	0.028	0.029	0.030	0.045

Table 2. Optical performance of a 40 inch meniscus mirror

GRAVITY LOAD	----- SURFACE DEFORMATION (RMS WAVE) -----				
	RING	12-30	6-60	4-90	3-120
ZENITH	0.071	0.071	0.105	0.253	0.614
HORIZON	0.009	0.010	0.011	0.019	0.083

Table 3. Comparison of double concaved mirrors, configurations 1 and 2

MIRROR SHAPE	GRAVITY LOAD	----- SURFACE DEFORMATION (RMS WAVE) -----				
		RING	12-30	6-60	4-90	3-120
CONFIG 1	ZENITH	0.282	0.284	0.292	0.402	0.883
Wt=467 LBS	HORIZON	0.002	0.003	0.008	0.012	0.020
CONFIG 2	ZENITH	0.646	0.649	0.653	0.775	1.473
Wt=343 LBS	HORIZON	0.002	0.002	0.007	0.011	0.020

Table 4. Optical performance of a 40 inch single arched mirror

MIRROR SHAPE	GRAVITY LOAD	----- SURFACE DEFORMATION (RMS WAVE) -----				
		RING	12-30	6-60	4-90	3-120
SINGLE ARCH	ZENITH	0.175	0.175	0.170	0.169	0.162
Wt=135 LBS	HORIZON	0.226	0.226	0.226	0.228	0.271

Table 5. 40 inch SXA mirror with $r/R_0=0.5$

MIRROR SHAPE	GRAVITY LOAD	----- SURFACE DEFORMATION (RMS WAVE) -----				
		RING	12-30	6-60	4-90	3-120
EQN 2-3	ZENITH	0.021	0.022	0.023	0.073	0.234
Wt=254 LBS	HORIZON	0.027	0.027	0.028	0.041	0.098
EQN 4-5	ZENITH	0.069	0.070	0.070	0.092	0.229
Wt=324 LBS	HORIZON	0.021	0.021	0.022	0.044	0.136
EQN 6-7	ZENITH	0.021	0.021	0.023	0.078	0.253
Wt=256 LBS	HORIZON	0.027	0.027	0.028	0.046	0.119

Table 6. 40 inch SXA mirror with $r/R_0=0.55$

MIRROR SHAPE	GRAVITY LOAD	----- SURFACE DEFORMATION (RMS WAVE) -----				
		RING	12-30	6-60	4-90	3-120
EQN 2-3	ZENITH	0.013	0.013	0.019	0.085	0.272
Wt=309 LBS	HORIZON	0.046	0.046	0.047	0.051	0.065
EQN 4-5	ZENITH	0.036	0.036	0.038	0.083	0.260
Wt=358 LBS	HORIZON	0.025	0.025	0.026	0.043	0.109
EQN 6-7	ZENITH	0.004	0.004	0.016	0.090	0.291
Wt=287 LBS	HORIZON	0.020	0.020	0.021	0.041	0.097

Table 7. 40 inch SXA mirror with $r/R_0=0.60$

MIRROR SHAPE	GRAVITY LOAD	----- SURFACE DEFORMATION (RMS WAVE) -----				
		RING	12-30	6-60	4-90	3-120
EQN 2-3	ZENITH	0.036	0.037	0.041	0.093	0.266
Wt=301 LBS	HORIZON	0.007	0.007	0.011	0.027	0.044
EQN 4-5	ZENITH	0.006	0.007	0.017	0.085	0.279
Wt=360 LBS	HORIZON	0.008	0.008	0.012	0.038	0.094
EQN 6-7	ZENITH	0.045	0.046	0.050	0.114	0.352
Wt=296 LBS	HORIZON	0.019	0.019	0.021	0.045	0.103

Table 8. 40 inch SXA mirror with $r/R_0=0.65$

MIRROR SHAPE	GRAVITY LOAD	----- SURFACE DEFORMATION (RMS WAVE) -----				
		RING	12-30	6-60	4-90	3-120
EQN 2-3	ZENITH	0.065	0.067	0.072	0.131	0.355
Wt=308 LBS	HORIZON	0.010	0.010	0.014	0.032	0.045
EQN 4-5	ZENITH	0.043	0.044	0.049	0.114	0.343
Wt=369 LBS	HORIZON	0.007	0.007	0.012	0.037	0.187
EQN 6-7	ZENITH	0.065	0.066	0.072	0.133	0.368
Wt=307 LBS	HORIZON	0.006	0.006	0.012	0.033	0.052
EQN 8-9	ZENITH	0.036	0.036	0.041	0.100	0.310
Wt=430 LBS	HORIZON	0.007	0.007	0.011	0.033	0.090

Table 9. Comparison between SXA and Fused Silica 40 inch mirrors with $r/R_0=0.5$ for (EQN 6-7).

MIRROR SHAPE	GRAVITY LOAD	----- SURFACE DEFORMATION (RMS WAVE) -----				
		RING	12-30	6-60	4-90	3-120
SXA	ZENITH	0.021	0.021	0.023	0.078	0.253
Wt=256 LBS	HORIZON	0.027	0.027	0.028	0.046	0.119
Fused Silica	ZENITH	0.021	0.022	0.025	0.097	0.322
Wt=235 LBS	HORIZON	0.041	0.041	0.042	0.060	0.149

Table 10. Optical performance of various contoured back shapes

MIRROR SHAPE	GRAVITY LOAD	----- SURFACE DEFORMATION (RMS WAVE) -----				
		RING	12-30	6-60	4-90	3-120
CONCAVE-FLAT	ZENITH	0.017	0.018	0.022	0.066	0.222
Wt=545 LBS	HORIZON	0.028	0.028	0.029	0.030	0.045
MENISCUS	ZENITH	0.071	0.071	0.105	0.253	0.614
Wt=620 LBS	HORIZON	0.009	0.010	0.011	0.019	0.083
DBL CONCAVE	ZENITH	0.282	0.284	0.292	0.402	0.883
Wt=467 LBS	HORIZON	0.002	0.003	0.008	0.012	0.020
SINGLE ARCH	ZENITH	0.175	0.175	0.170	0.169	0.162
Wt=135 LBS	HORIZON	0.226	0.226	0.226	0.228	0.271
DOUBLE ARCH	ZENITH	0.036	0.037	0.041	0.093	0.266
Wt=301 LBS	HORIZON	0.007	0.007	0.011	0.027	0.044

Table 11. Optical deformation of 16 inch solid single arch mirror

MIRROR ID	HORIZON (RMS wave)	ZENITH (RMS wave)	WEIGHT (LBS)
SXA13	0.003	0.004	18.9
SXA14	0.003	0.007	27.3
SXA15	0.007	0.009	35.6
SXA23	0.016	0.022	13.0
SXA24	0.006	0.010	21.3
SXA25	0.003	0.015	29.6
SXA29	0.017	0.018	13.5
SXA30	0.003	0.012	16.2

Table 12. Optical deformation of 16 inch foam core single arch mirror

MIRROR ID	HORIZON (RMS wave)	ZENITH (RMS wave)	MIRROR Wt. (LBS)	FOAM Wt. TOTAL Wt.
SW27	0.028	0.183	6.8	0.22
SW28	0.024	0.189	7.3	0.27
SW29	0.022	0.251	7.8	0.31
SW30	0.025	0.148	7.0	0.21
SW31	0.027	0.227	7.5	0.28
SW40	0.048	0.218	6.4	0.16